

Erasing Self-Supervised Learning Backdoor by Cluster Activation Masking

Shengsheng Qian^{1,2} Yifei Wang³ Dizhan Xue^{1,2} Shengjie Zhang³ Huaiwen Zhang⁴ Changsheng Xu^{1,2,5}

¹MAIS, Institute of Automation, Chinese Academy of Sciences

²University of Chinese Academy of Sciences

³Zhengzhou University

⁴College of Computer Science, Inner Mongolia University

⁵Peng Cheng Laboratory

shengsheng.qian@nlpr.ia.ac.cn, wang-fei@gs.zzu.edu.cn, xuedizhan17@mails.ucas.ac.cn

zsj2021@gs.zzu.edu.cn, huaiwen.zhang@imu.edu.cn, csxu@nlpr.ia.ac.cn

Detection ACC	PatchSearch (based on Grad-CAM)	PoisonCAM (Ours)	Detection ACC
TOP 20 10%			TOP 20 95%
TOP 50 6%			TOP 50 96%
TOP 100 3%			TOP 100 96%

Figure 1. Retrieved backdoor trigger patches from the poisoned ImageNet-100 (poison rate 0.5%, target category “rottweiler”) by PatchSearch (left) [49] and our PoisonCAM (right).

Abstract

Researchers have recently found that Self-Supervised Learning (SSL) is vulnerable to backdoor attacks. The attacker can embed hidden SSL backdoors via a few poisoned examples in the training dataset and maliciously manipulate the behavior of downstream models. To defend against SSL backdoor attacks, a feasible route is to detect and remove the poisonous samples in the training set. However, the existing SSL backdoor defense method fails to detect the poisonous samples precisely. In this paper, we propose to erase the SSL backdoor by cluster activation masking and propose a novel PoisonCAM method. After obtaining the threat model trained on the poisoned dataset, our method can precisely detect poisonous samples based on the as-

sumption that masking the backdoor trigger can effectively change the activation of a downstream clustering model. In experiments, our PoisonCAM achieves 96% accuracy for backdoor trigger detection compared to 3% of the state-of-the-art method on poisoned ImageNet-100. Moreover, our proposed PoisonCAM significantly improves the performance of the trained SSL model under backdoor attacks compared to the state-of-the-art method. Our code, poisoned datasets, and trained models will be open once this paper is accepted.

1. Introduction

In recent years, Self-Supervised Learning (SSL) [20, 26, 30, 33, 44] has emerged as a powerful paradigm in machine

learning, enabling models to learn from vast amounts of unlabeled data. Without the reliance on manual feature engineering or human annotations, SSL is able to learn meaningful representations from unlabeled data and facilitate a range of downstream tasks, such as clustering and classification [5, 7, 8, 15, 17]. However, recent work [2, 43] has found that SSL is vulnerable to backdoor attacks where an attacker can inject a stealthy backdoor trigger into SSL models by poisoning a small number of training samples.

SSL backdoor attacks [2] pose a significant challenge to the security and robustness of SSL models, of which the procedure can be summarized as follows: First, an attacker selects a stealthy backdoor trigger for a specific target category. Next, the attacker injects the trigger patch into some data of the target category. After training on the poisoned dataset, the SSL model will construct a strong correlation between the trigger and the target category. Finally, the attacker can manipulate the behavior of the downstream model by attaching the trigger to the input, such as forcing the downstream classifier to misclassify the image as the target category. Meanwhile, the attacked model can behave similarly to unattacked models when the trigger is absent in the input, making the injected backdoor stealthy. Facing the threat of SSL backdoor attacks, this work aims to erase the SSL backdoor and train a trustworthy SSL model. For practicability, we assume that the defender has no prior knowledge of the trigger or target category, and lacks access to trusted data, following [29, 34, 36, 38, 49].

To defend against SSL backdoor attacks, a feasible and straightforward route is to detect and remove the poisonous samples in the training set. However, since semantic annotations are unavailable in SSL, detecting the backdoor trigger is not a trivial problem and should be achieved in a totally unsupervised manner. The existing method [49] (i.e., PatchSearch) utilizes Grad-CAM [45] on a downstream clustering model to retrieve trigger patches injected into the dataset, based on which a poison classifier is trained to classify poisonous or clean data. However, as shown in Figure 1, the accuracy of top 20, top 50, and top 100 trigger patches retrieved by PatchSearch are only 10%, 6%, and 3% on the poisoned ImageNet-100. Subsequently, PatchSearch is limited in distinguishing between trigger patches and benign patches, reducing the effectiveness of the finally trained SSL models. Therefore, this work focuses on addressing a major challenge in SSL backdoor defense: How to accurately retrieve the SSL backdoor trigger patches injected in a poisoned and unlabeled dataset?

In this paper, we propose PoisonCAM, which aims at accurately detecting poisonous samples in a poisoned and unlabeled dataset to erase the SSL backdoor. To retrieve the trigger patches injected into the poisoned dataset, we propose a novel Cluster Activation Masking method. Our method is based on the assumption that masking a success-

ful trigger in an image will change the cluster assignment from the target category of the trigger to the true category of the image. Therefore, the trigger patches can be detected by comparing the cluster activation under a few random masks. As shown in Figure 1, our PoisonCAM significantly improves the top 20, 50, and top 100 accuracy of the retrieved trigger patches from 10%, 6%, and 3% of the state-of-the-art PatchSearch to 95%, 96%, and 96% on the poisoned ImageNet-100. Based on the more accurate trigger patches, our trained poison classifier also significantly improves the precision of detecting poisonous samples from 5.4% to 49.3% while achieving even higher recall (see details in Table 2). Finally, after accurately detecting and removing the poisonous samples, the trained SSL model on the clean-up dataset achieves new state-of-the-art results in terms of both the performance and the backdoor defense.

In brief, the contributions of this work are summarized as follows:

- We propose PoisonCAM, a novel SSL backdoor defender model, to accurately detect and remove poisonous data from a poisoned and unlabeled dataset. Subsequently, an effective and backdoor-free SSL model can be trained on the clean-up dataset.
- We propose a Cluster Activation Masking method to accurately retrieve trigger patches injected into the poisoned dataset. Based on the retrieved trigger patches, an effective poison classifier is trained to classify poisonous or clean data in the training set.
- Extensive experimental results on ImageNet-100 and STL-10 demonstrate that our proposed PoisonCAM significantly outperforms the state-of-the-art method for defending against SSL backdoor attacks.

2. Related Work

Self-Supervised Learning. The objective of self-supervised learning (SSL) [12, 14, 35, 52, 57] is to acquire representations from uncurated and unlabeled data through a pretext task that is derived from the data itself, without any human annotations. MoCo [7, 8, 17] is a widely employed contrastive SSL algorithm that involves classifying two augmented versions of the same image as positive pairs, which are then contrasted to negative pairs consisting of augmentations from different images. Contrastive SSL algorithms are further explored in [3, 5, 10, 46, 56]. BYOL [15] is a non-contrastive SSL algorithm that predicts the target network representation of the same image under a different augmented view without negatives. Non-contrastive SSL algorithms are further developed in [6, 23–25, 54]. Despite the remarkable potential, SSL algorithms are not immune to vulnerabilities. In this paper, we study the defense against backdoor attacks on SSL to promote trustworthy and reliable SSL models.

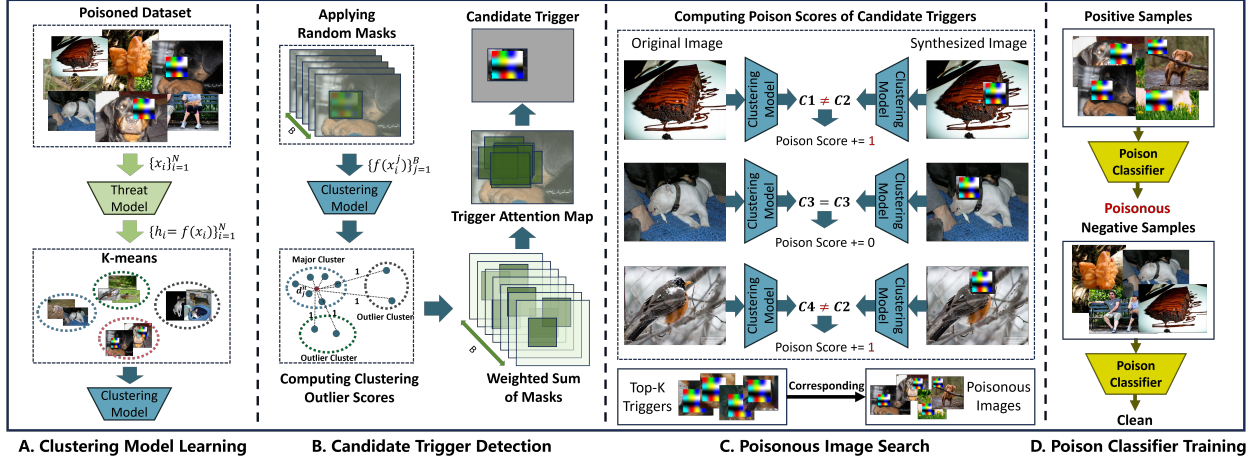


Figure 2. The overview of PoisonCAM: (1) Learn a clustering model on the poisoned dataset by k -means algorithm; (2) Detect the candidate trigger in each image based on clustering outlier scores of random masks and the weighted sum of masks as the trigger attention map; (3) Compute the poison scores of candidate triggers and retrieve the top- k triggers with corresponding poisonous images; (4) Train a poison classifier to identify and remove poisonous samples in the poisoned dataset.

SSL Backdoor Attacks. The purpose of SSL backdoor attacks is to inject a stealthy backdoor trigger into SSL models by poisoning training data, which can be activated to manipulate the behavior of downstream models at test time [21, 48]. Saha et al. [43] propose backdoor attacks towards SSL models by attaching a trigger patch to images of a target category. At test time, the downstream classifier has high accuracy on clean images but misclassifies images with the trigger as the target category. The authors also propose a distillation-based defender, which requires a substantial amount of trusted data and may be infeasible in real-world scenarios. Li et al. [27] recently propose a similar SSL backdoor attack method. The key difference is that they adopt a frequency domain based spectral trigger to resist the data augmentations. Carlini and Terzis [2] propose backdoor attacks towards CLIP [39], a multimodal contrastive SSL model. Their attack is implemented by injecting triggers into the victim images and tampering with the paired textual captions.

SSL Backdoor Defenses. Despite the prosperity of backdoor defense for supervised learning [19, 32, 53, 58, 60], SSL backdoor defense is a relatively under-explored and more challenging problem. Tejankar et al. [49] explore to defend against patch-based SSL backdoor attacks [43]. Their method adopts Grad-CAM [45] on a clustering model to detect candidate triggers and train a poison classifier to identify and delete poisonous samples in the training data. However, they compromisingly delete a large amount of clean samples due to the low accuracy of their poison classifier. Bansal et al. [1] propose to defend the multimodal SSL backdoor attacks on CLIP. They find that simply integrating an intra-modal contrastive loss can effectively mitigate

multimodal SSL backdoor attacks. **In this paper, we follow the research line of patch-based SSL backdoor attacks on visual SSL models [43, 49] due to their substantial feasibility and destructiveness.** We propose a novel PoisonCAM method based on Cluster Activation Masking to detect and delete the poisonous samples in the training set while deleting as few clean samples as possible.

3. Threat Model

We introduce the threat model under the SSL backdoor attack proposed in [43]. The primary objective of the attacker is to manipulate the output of a downstream model which is constructed based on the SSL model. In this paper, we take a downstream image classifier as the example, following previous work [43, 49]. Assume that an unlabeled poisoned dataset $\mathbf{X} = \{x_i \in \mathbb{R}^{C \times H \times W}\}_{i=1}^N$ contains N images where x_i is the i -th image, C denotes the number of channels, H and W denote the height and the width of an image, respectively. The attacker’s purpose is two-fold. Firstly, the attacker aims to surreptitiously implant a backdoor into an SSL model, enabling the downstream classifier to misclassify an incoming image as the target category if the image contains the attacker-designated trigger t . Secondly, the attacker seeks to hide the backdoor’s presence by ensuring that the performance of the downstream classifier is similar to that of a classifier based on an unattacked SSL model when the trigger is absent. The attacker’s objectives can be achieved through a technique known as “data poisoning”. This involves the attachment of a small trigger patch to a few images of the preselected target category. The attacker posits that the SSL algorithm associates the trigger with the target category, resulting in a successful at-

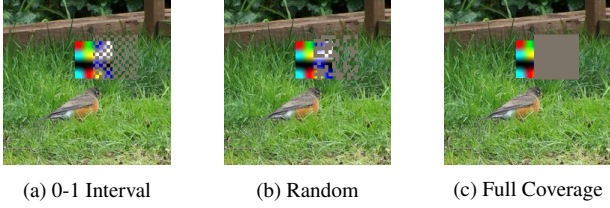


Figure 3. An example of three masking strategies.

tack. Then, the model $f(\cdot)$ trained on the poisoned dataset \mathbf{X} via SSL algorithms (e.g., MoCo [7, 8, 17]) is defined as the threat model. Moreover, the learned feature $\mathbf{h}_i = f(x_i)$ can be utilized in the downstream tasks.

4. Proposed Defender Model

The objective of the defender model is to remove the SSL backdoor, eliminating the hidden correlation between the attacker-designed trigger and the target category. Simultaneously, the defender should avoid impairing the model’s performance on clean data. To enhance the practicability, we assume that the defender should achieve this without any prior knowledge of the trigger or target category, and lacking access to trusted data, following [29, 34, 36, 38, 49].

In this section, we propose our defender model named PoisonCAM, which aims at identifying the poisonous samples in the training set and filtering them out to form a clean-up training dataset $\bar{\mathbf{X}} \subset \mathbf{X}$. The overall architecture of our method is shown in Figure 2, which mainly consists of four steps: (1) Learning clustering model for the poisoned dataset \mathbf{X} ; (2) Detect the candidate triggers for all images in \mathbf{X} ; (3) Search for the top- k poisonous samples with the highest poison scores; (4) Train a poison classifier to find and delete all poisonous samples in \mathbf{X} . Subsequently, the clean-up training dataset $\bar{\mathbf{X}}$ can be formed and a backdoor-free SSL model can be trained on $\bar{\mathbf{X}}$.

4.1. Clustering Model Learning

Due to the lack of labels in SSL, we first learn a clustering model $C(\cdot)$ for features $\{f(x_i)\}_{i=1}^N$ by k -means algorithm [31] to capture the semantics of training data, as follows:

$$y_i = C(f(x_i)), \quad (1)$$

where $y_i \in \{1, \dots, l\}$ represents the corresponding cluster label and l is a hyper-parameter. Since the threat model is sensitive to triggers, the poisonous images with triggers will tend to be classified into a cluster of triggers. The clustering model $C(\cdot)$ is fixed and will be utilized in the following.

4.2. Candidate Trigger Detection for Images

In candidate trigger detection, we aim to detect the candidate trigger region in every image x_i . The state-of-the-art PatchSearch [49] employs Grad-CAM [45] to detect the

pivotal region of an image x_i for clustering as the candidate trigger region. However, previous work [4, 22, 51] has found that Grad-CAM may fail to locate the pivotal region for the downstream tasks. Moreover, as we empirically show the detection results on poisoned ImageNet-100 in Figure 1 (a), Grad-CAM suffers from detecting the trigger in this poisoned SSL dataset. Therefore, we propose a novel Cluster Activation Masking method based on the assumption that masking a trigger t in an image x_i will change the cluster assignment y_i from the cluster of triggers to the true cluster of x_i . By analyzing the cluster activation under B different random masks, we can locate the candidate trigger t_i in x_i .

Specifically, using the obtained clustering model $C(\cdot)$ in Equation 1, we aim at locating the region of the potential trigger in x_i . For any image $x_i \in \mathbf{X}$, we randomly initialize B masks $\mathbf{M} = \{\mathbf{m}_j \in \{0, 1\}^{H \times W}\}_{j=1}^B$. In particular, we set the pixel value to zero if the corresponding mask value is 1 and keep the pixel value unchanged if the corresponding mask value is 0. After randomly selecting a masking window of the size of $[w, w]$, we have empirically tested three masking strategies, as shown in Figure 3. Although it seems that 0-1 Interval Masking and Random Masking can break the pattern of the trigger while protecting the semantics of benign regions, we empirically found in experiments (see Section 5.7) that Full Coverage Masking is the optimal strategy. We apply masks $\{\mathbf{m}_j\}_{j=1}^B$ to obtain B degraded images $\mathbf{D} = \{x_i^j = x_i \odot (1 - \mathbf{m}_j)\}_{j=1}^B$, where \odot denotes the element-wise multiplication. Then we classify the features of \mathbf{D} by the clustering model $C(\cdot)$ to get cluster labels $\{\eta_j = C(f(x_i^j))\}_{j=1}^B$ and the distances to the assigned cluster centers $\{d_j\}_{j=1}^B$. Since the size of the backdoor trigger is much smaller than the whole image, most masks cannot change the clustering assignment of x_i^j . Therefore, most samples from \mathbf{D} are assigned to the same cluster and we denote this cluster as η^* . To scale cluster distances, we utilize Max-Min Scaling to normalize d_j as $d_j^n = \frac{d_j - \min_k d_k}{\max_k d_k - \min_k d_k} \in [0, 1]$. Then, we compute the clustering outlier score a_j of the mask \mathbf{m}_j as follows:

$$a_j = \begin{cases} d_j^n & \eta_j = \eta^* \\ 1 & \eta_j \neq \eta^* \end{cases} \quad (2)$$

For a poisonous sample x_i , η^* should be the target category of trigger t . $\eta_j \neq \eta^*$ means the trigger is successfully masked. When the trigger is not successfully masked, larger d_j^n to the cluster center η^* means more region of the trigger is masked. Therefore, a_j can represent the importance score of successfully masking the trigger. Based on the scores $\{a_i\}_{i=1}^B$, the masks are aggregated through weighted sum-

mation to obtain an attention map of the trigger, as follows:

$$A = \frac{\sum_{j=1}^B \mathbf{m}_j \times a_j}{\sum_{j=1}^B \mathbf{m}_j} \in \mathbb{R}^{H \times W}, \quad (3)$$

where A is the attention map of the trigger, and the value A_{mn} positively correlates to the presence possibility of the trigger. After obtaining the attention map of the image x_i , we select the window t_i of size $w \times w$ with the largest sum attention value in the window. Therefore, t_i can be regarded as the optimal window of the potential trigger t in x_i and we denote t_i as the candidate trigger for simplicity.

4.3. Poisonous Image Search

In this section, we aim to find a set of highly poisonous images in \mathbf{X} . To quantify the poisonousness of a given image x_i , we define the poison score of x_i . Our method is based on the assumption that pasting a real trigger onto an image will strongly change its clustering assignment while the effectiveness of pasting a benign region is much weaker. Specifically, we first obtain a fixed test set \mathbf{X}^f by sampling a few images per cluster that are closest to their respective cluster centers. Subsequently, we paste the candidate trigger t_i onto all images in \mathbf{X}^f and get their new cluster assignments. Finally, the poison score of x_i is calculated as the number of images in \mathbf{X}^f whose cluster assignments are changed after pasting the candidate trigger t_i .

To find a few highly poisonous images, we can compute the poison scores of all images and simply take the top- k image as the poisonous samples. However, to improve the efficiency and utilize the clustering information of images, we adopt a heuristic search strategy following [49] to iteratively compute poison scores for a part of (not all) images in \mathbf{X} . Finally, we take the top- k scored images with the highest poison scores to form a poison set \mathbf{X}^p . This poison set will be utilized to train a classifier of poisonous samples.

4.4. Poison Classifier Training

Aiming at precisely detecting all poisonous samples in \mathbf{X} , we train a ResNet [16] as the poison classifier. Specifically, for every $x_i \in \mathbf{X}$, we randomly select a sample x_k in the poison set \mathbf{X}^p and paste its candidate trigger t_k at a random location on x_i . These synthesized images as the positive samples and original images in \mathbf{X} as the negative samples form the poison classification set $\tilde{\mathbf{X}}$. Since poisonous samples from \mathbf{X} are noisy for poison classification, we eliminate a proportion p of images with the highest poison scores in \mathbf{X} and utilize strong augmentations and early stopping to alleviate the noisy problem. Then, the poison classifier trained on $\tilde{\mathbf{X}}$ is applied to \mathbf{X} , and all images classified as ‘‘poisonous’’ are removed to form a clean-up training dataset $\bar{\mathbf{X}}$. Finally, after erasing the SSL backdoor in the poisoned dataset, we can train a benign SSL model on $\bar{\mathbf{X}}$,

which can achieve similar performance to the threat model $f(\cdot)$ on clean samples but will not be manipulated by the attacker-designated trigger.

5. Experiments

We include implementation details and more experimental results in Supplementary Material.

5.1. Datasets

Following previous work [49], we adopt **ImageNet-100** [50], which contains images belonging to 100 randomly sampled classes from the 1000 classes of ImageNet [41]. The training set has about 127K samples and the validation set has 5K samples. **STL-10** [11] contains 500/800 training/validation images for each of 10 classes.

5.2. Attack Setting

Following the SSL backdoor attacks proposed in [43], we randomly adopt 10 different target categories and trigger patches. In every experiment, we set a single target category and use a single trigger patch. On ImageNet-100, we set the poisoning rates as 0.5% and 1.0%, which mean 50% and 100% images of the target category being poisoned to form a poisonous dataset. On STL-10, we set the poisoning rates as 5.0%, which mean 50% images of the target category being poisoned. The HTBA triggers [42, 47] are pasted with size 50×50 onto the images and 25% of the edges is reserved on four sides of the images. After injecting the triggers, we train a threat model on the poisoned dataset \mathbf{X} . Following PatchSearch [49], we adopt ViT-B [13] as the backbone with MoCo-v3 algorithm [8] to train threat models on poisoned datasets.

5.3. Baseline Method and Evaluation Metrics

We adopt the state-of-the-art SSL defense method PatchSearch [49] and the naive method without defense as the baseline methods. We fairly compare our proposed Poison-CAM with baselines by sharing the weights of the threat model. For the evaluation, we train a linear classifier on a trained SSL model by randomly sampling a 1.0% subset from the clean labeled training dataset, following PatchSearch. Since PatchSearch has not released its trained models, we reimplement PatchSearch using the official code¹. We will release our poisoned datasets, code, and trained models once this paper is accepted.

We denote the original validation set of ImageNet-100 as the clean validation set, which consists of 50 randomly selected images from each category, and form a poisoned validation set by randomly pasting the attacked trigger on the images of the clean validation set. Similarly, we construct the clean and poisoned validation sets of STL-10. We then

¹<https://github.com/UCDvision/PatchSearch>

Table 1. **Defense results.** We compared the performance of the attacked SSL models with different defense methods under various attack settings on the validation set. ACC denotes accuracy. ASR denotes attack success rate. Clean Val denotes the clean validation set and Poisoned Val denotes the poisoned validation set.

Attack Settings		w/o Defense				PatchSearch				PoisonCAM			
Dataset	Target Category	Clean Val		Poisoned Val		Clean Val		Poisoned Val		Clean Val		Poisoned Val	
		ACC \uparrow	ASR \downarrow	ACC \uparrow	ASR \downarrow	ACC \uparrow	ASR \downarrow	ACC \uparrow	ASR \downarrow	ACC \uparrow	ASR \downarrow	ACC \uparrow	ASR \downarrow
ImageNet-100 (poison rate 0.5%)	rottweiler	69.4	0.5	27.7	63.9	68.0	0.5	61.9	0.4	70.6	0.5	65.2	0.5
	tabby cat	69.1	0.0	30.2	61.8	67.3	0.0	60.7	0.1	70.9	0.1	64.7	0.1
	ambulance	69.4	0.0	57.3	9.6	66.6	0.0	56.5	3.5	69.4	0.1	62.3	0.1
	pickup truck	70.1	0.3	58.5	9.3	65.6	0.4	60.2	0.3	71.0	0.3	65.4	0.3
	laptop	69.2	0.9	38.0	52.4	66.2	1.0	48.9	24.5	68.9	0.8	61.6	2.4
	goose	69.4	0.2	44.7	35.5	66.8	0.2	61.1	0.3	70.0	0.2	63.4	0.3
	pirate ship	69.5	0.0	52.5	22.2	66.0	0.1	51.8	15.1	68.5	0.1	61.5	0.2
	gas mask	68.6	0.3	33.4	58.8	69.4	1.1	63.1	2.1	68.8	0.9	63.3	2.1
	vacuum cleaner	69.1	1.1	44.0	32.2	67.8	1.2	61.0	1.1	70.0	1.4	62.7	1.2
	American lobster	68.8	0.1	44.0	42.5	65.2	0.3	59.6	0.3	69.2	0.2	62.4	0.2
	average	69.3	0.3	43.0	38.8	66.9	0.5	58.5	4.8	69.7	0.4	63.2	0.7
ImageNet-100 (poison rate 1.0%)	rottweiler	69.4	0.4	26.2	70.9	67.1	0.5	60.9	0.5	69.3	0.7	63.5	0.6
	tabby cat	69.3	0.0	25.8	69.9	68.0	0.5	62.8	0.7	68.7	0.5	63.4	0.6
	ambulance	69.5	0.0	49.4	23.3	67.0	0.2	58.1	2.3	69.9	0.2	62.4	0.4
	pickup truck	69.2	0.3	52.6	22.4	67.6	0.4	61.8	0.4	69.0	0.4	63.2	0.5
	laptop	69.0	0.8	31.6	61.4	69.0	1.1	61.5	3.4	69.4	0.9	62.7	1.3
	goose	69.7	0.2	40.0	47.8	61.9	0.4	56.5	0.4	68.3	0.5	61.7	0.6
	pirate ship	69.0	0.1	49.1	30.8	68.8	0.5	60.9	4.0	68.9	0.4	61.8	0.8
	gas mask	68.7	0.3	29.2	65.4	68.2	1.3	60.4	4.3	69.1	1.3	62.5	2.3
	vacuum cleaner	68.9	1.0	39.2	44.5	69.0	1.3	61.0	2.1	69.9	1.4	63.3	1.4
	American lobster	69.0	0.1	27.2	68.1	67.9	0.7	61.7	1.9	69.9	0.6	62.5	2.1
	average	69.2	0.3	37.0	50.4	67.4	0.7	60.6	2.0	69.2	0.7	62.7	1.1
STL-10 (poison rate 5.0%)	bird	63.2	5.1	50.8	28.7	62.6	3.1	56.2	7.1	65.4	4.9	61.0	5.1
	car	62.0	1.8	41.2	41.3	61.8	1.8	40.8	3.3	62.8	1.1	43.6	3.1
	deer	65.8	2.9	43.8	25.1	64.0	3.3	42.2	4.8	63.8	4.0	51.0	4.2
	average	63.7	3.3	45.3	31.7	62.8	2.7	46.4	5.1	64.0	3.3	51.9	4.1

assess the results both on the clean validation set and the poisoned validation set by using the following metrics: Accuracy (ACC) and Attack Success Rate (ASR) [28, 55, 59] for the attacked class. Attack Success Rate (ASR) refers to the proportion of non-target classes misclassified by the classifier as the targeted class. All results are averaged over 5 independent runs with different seeds.

5.4. Results and Discussions

The results on poisoned ImageNet-100 and STL-10 under different attack settings are shown in Table 1. Based on the results, we have the following observations:

- Our proposed PoisonCAM significantly outperforms baselines against SSL backdoor attacks. Specifically, on poisoned validation sets, PoisonCAM achieves average ACC improvements of 4.7%, 2.1%, and 5.5% and average ASR reductions of 4.1%, 0.9%, and 1.0% on ImageNet-100 (poison rate 0.5%), ImageNet-100 (poison rate 1.0%), and STL-10 (poison rate 5.0%), respectively. These results indicate that PoisonCAM can better defend against backdoor attacks by accurately removing

poisonous samples for detoxified training.

- Our PoisonCAM achieves similar or even higher ACC than w/o Defense on clean validation sets where backdoor triggers are absent. Compared to PatchSearch, PoisonCAM achieves 2.8%, 1.8%, and 1.2% average ACC improvements on ImageNet-100 (poison rate 0.5%), ImageNet-100 (poison rate 1.0%), and STL-10 (poison rate 5.0%), respectively while achieving similar ASRs. This is because PoisonCAM can classify poisonous samples more accurately and delete fewer benign samples to facilitate sufficient training. Since PatchSearch deletes too many clean samples, its ACC obviously declines compared to w/o Defense on three datasets.

5.5. Analysis of Poisonous Image Detection

A key step in PatchSearch and our PoisonCAM is to detect poisonous images in the training set and remove them. To further investigate the effectiveness of our method, we analyze the results of poisonous image detection by PoisonCAM and PatchSearch. In Table 2, we report the number of total removed images (Total Rem.), recall, and precision on

Table 2. **Poison detection results.** We compare the average results over target categories for detecting poisonous images in the poisoned datasets. *Total Rem.* denotes the number of total removed samples.

Dataset	Metric	PatchSearch	PoisonCAM
ImageNet-100 (poison rate 0.5%)	Total Rem.	12807.5	1570.8
	Recall↑	84.4	98.7
	Precision↑	5.4	49.3
ImageNet-100 (poison rate 1.0%)	Total Rem.	10740.7	2214.9
	Recall↑	99.0	99.1
	Precision↑	20.9	64.3
STL-10 (poison rate 5.0%)	Total Rem.	744.0	332.0
	Recall↑	98.5	99.1
	Precision↑	62.5	78.6

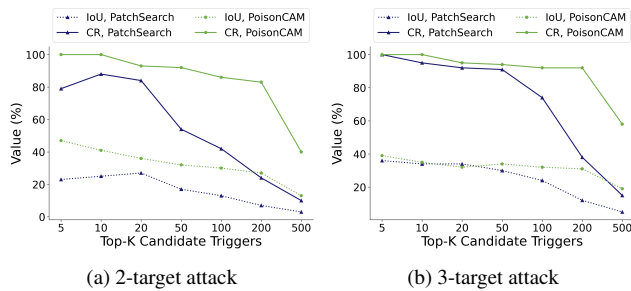


Figure 4. Results of the detected top- k candidate triggers by PatchSearch and our PoisonCAM against multi-target attacks.

three datasets. We have the following observations:

- Compared to PatchSearch, our PoisonCAM significantly improves average precision by 43.9%, 43.4%, and 16.1% on ImageNet-100 (poison rate 0.5%), ImageNet-100 (poison rate 1.0%), and STL-10 (poison rate 5.0%), respectively. These results demonstrate that PoisonCAM can detect poisonous images more accurately and reduce mistakenly removed benign samples, which also results in the lower Total Rem. Subsequently, PoisonCAM can facilitate more sufficient training to improve the performance of the SSL models.
- Moreover, PoisonCAM achieves similar or higher recall compared to PatchSearch on three datasets. Especially, the recall of PoisonCAM is always higher than 95% on all datasets. As a result, PoisonCAM can remove poisonous samples more effectively and facilitate detoxified SSL training.

We include the detailed results of every target category in Supplementary Material.

5.6. Results of Multi-Target Attacks

To further investigate the effectiveness of different methods, we conduct experiments against multi-target attacks. Specifically, we utilize multiple target categories and correlate different backdoor triggers to different target cate-

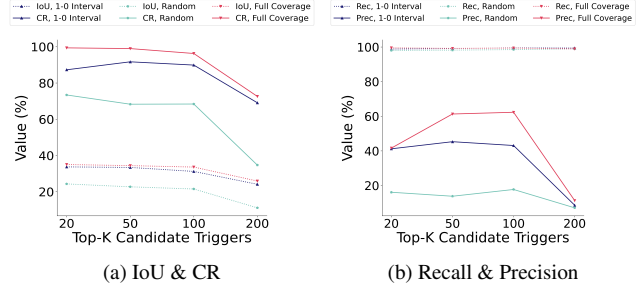


Figure 5. Ablation study on different masking strategies on ImageNet-100 (poison rate 0.5%, target category “rottweiler”). Rec., Prec. denotes Recall and Precision.

gories. We combine target categories of “rottweiler” and “tabby cat” to conduct 2-target attacks, and further add “ambulance” to conduct 3-target attacks on ImageNet-100 (poison rate 0.5%). As shown in Figure 4, we report the results of top- k retrieved candidate triggers by PatchSearch and PoisonCAM. We introduce two metrics, Intersection over Union (IoU) [9, 40], and Catch Rate (CR). IoU measures the union divided by the intersection between the real triggers and the retrieved triggers. CR measures the ratio of the real triggers contained in the retrieved triggers.

We have the following observations: (1) Our PoisonCAM significantly outperforms PatchSearch against multi-target attacks. For example, PoisonCAM always achieves the best CR with every search number from top-5 to top-500. These results show that PoisonCAM can locate larger trigger areas than PatchSearch, which facilitates training a more accurate poison classifier to identify poisonous samples. (2) CR and IoU of both methods decline with the search number increasing from top-5 to top-500. However, diverse candidate triggers are also necessary for capturing the global characteristics of the real triggers. Therefore, an appropriate search number should be selected to balance the accuracy and diversity of the detected triggers.

5.7. Ablation Study

To further investigate the effectiveness of the designed masking strategies in Section 4.2, we design different masking strategies and conduct an ablation study on ImageNet-100 (poison rate 0.5%) with the target category “rottweiler”: Recalling that we set the size of masking windows as $[w, w]$, we compare three masking strategies:

- 0-1 Interval Masking: A block is defined with a size of $[w', w'] (w' \ll w)$. The entire window is evenly divided into blocks. Every block is assigned a value of 0 or 1, *s.t.*, every two adjacent blocks are assigned different values, as shown in Figure 3 (a).
- Random Masking [18]: Again, the entire window is evenly divided into blocks. Half of the blocks are randomly selected and assigned a value of 0, others are as-

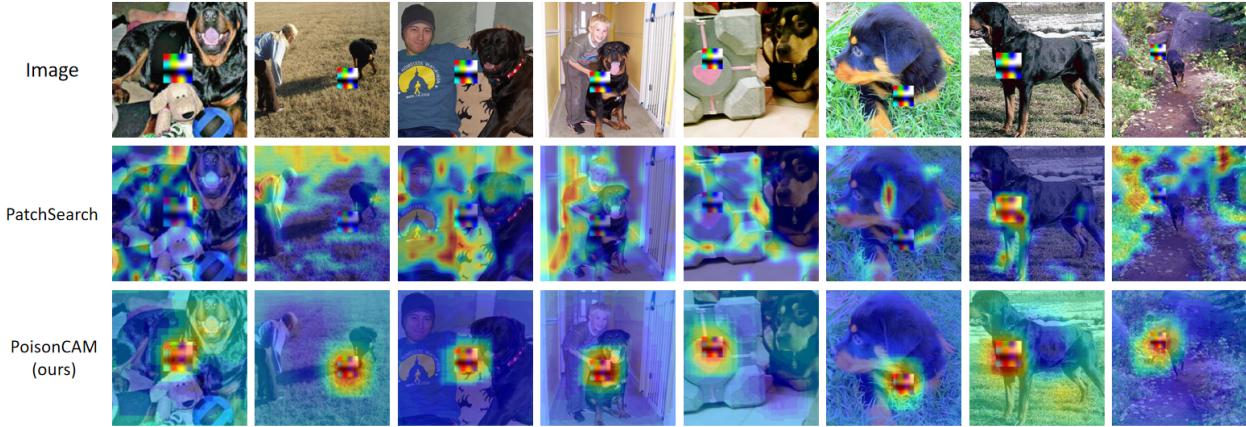


Figure 6. Visualization of trigger attention maps generated by PatchSearch and our PoisonCAM on ImageNet-100 (poison rate 0.5%, target category “rottweiler”).

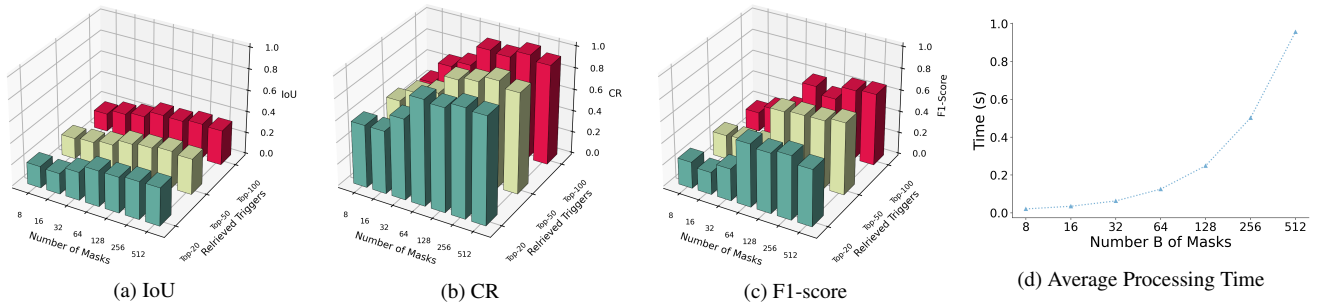


Figure 7. Hyper-parameter sensitivity study on the number B of masks on ImageNet-100 (poison rate 0.5%, target category “rottweiler”). (a-b) IoU and CR of the detected candidate triggers. (c) F1-score of the trained poison classifier. (d) Average processing time per image of candidate trigger detection.

signed a value of 1, as shown in Figure 3 (b).

3. Full Coverage Masking: The entire window is assigned a value of 1, as shown in Figure 3 (c).

As we report the results in Figure 5, we have the following observations: (1) Full Coverage Masking achieves both the highest IoU and CR among all strategies and can catch nearly the entire ($\sim 100\%$ CR) trigger regions with the search number from top-20 to top-100. (2) Simultaneously, the trained poison classifier with Full Coverage Masking achieves the highest precision and nearly 100% recall with different search numbers. Based on these observations, we empirically select Full Coverage Masking in our method.

5.8. Analysis of Trigger Attention Maps

To further investigate the process of two defenders, PoisonCAM and PatchSearch, we conduct a qualitative analysis of the generated trigger attention maps. Both methods generate trigger attention maps for images and select the hottest regions as the candidate triggers. PatchSearch adopts Grad-CAM [45] to compute the trigger attention, while we propose a Cluster Activation Masking method in Section 4.2

to solve this problem. Therefore, we visualize the cases of trigger attention maps generated by PoisonCAM and PatchSearch on ImageNet-100 (poison rate 0.5%) with the target category “rottweiler” in Figure 6. Our method can always accurately locate the backdoor triggers contained in these images, while PatchSearch focuses on more dispersed and maybe irrelevant regions. These results further demonstrate that our PoisonCAM can significantly improve the detection accuracy of the injected backdoor trigger, which is fundamental for defending against SSL backdoor attacks.

5.9. Hyper-parameter Sensitivity Study

In this section, we analyze the number B of masks in terms of sensitivity with the search number from top-20 to top-100 on ImageNet-100 (poison rate 0.5%) with the target category “rottweiler”. As demonstrated in Figure 7, we have the following observations: (1) While increasing the number B of masks, IoU, CR of the detected candidate triggers and F1-score of the trained poison classifier first increase and then become relatively stable, which shows that our method can effectively locate the triggers with appropriate

large B . The searching time increases with more masks to calculate. (2) The average processing time consistently increases while the number B of masks increases. Considering the worst situation where all masks are processed serially, the slope of the time curve will tend towards a constant. To conclude, an appropriate value of B should be chosen to balance the performance and time costs. We empirically set $B = 256$ in our method.

6. Conclusion

In this paper, we propose a novel PoisonCAM method to defend against self-supervised learning (SSL) backdoor attacks. PoisonCAM exhibits a robust capacity to accurately detect and remove poisonous data from a poisoned and unlabeled dataset to facilitate detoxified SSL training. We propose a Cluster Activation Masking method to accurately retrieve trigger patches injected into the poisoned dataset. Based on the retrieved trigger patches, an effective poison classifier is trained to distinguish between poisonous and clean data in the training set. Extensive experiments on ImageNet-100 and STL-10 demonstrate that PoisonCAM outperforms the state-of-the-art method for defending against SSL backdoor attacks. We hope this paper can contribute to the safety of artificial intelligence systems.

References

- [1] Hritik Bansal, Nishad Singhi, Yu Yang, Fan Yin, Aditya Grover, and Kai-Wei Chang. Cleanclip: Mitigating data poisoning attacks in multimodal contrastive learning. In *ICLR 2023 Workshop on Trustworthy and Reliable Large-Scale Machine Learning Models*, 2023. 3
- [2] Nicholas Carlini and Andreas Terzis. Poisoning and backdooring contrastive learning. In *International Conference on Learning Representations*, 2021. 2, 3
- [3] Mathilde Caron, Ishan Misra, Julien Mairal, Priya Goyal, Piotr Bojanowski, and Armand Joulin. Unsupervised learning of visual features by contrasting cluster assignments. In *Proceedings of the 34th International Conference on Neural Information Processing Systems*, Red Hook, NY, USA, 2020. Curran Associates Inc. 2
- [4] Aditya Chattopadhyay, Anirban Sarkar, Prantik Howlader, and Vineeth N Balasubramanian. Grad-cam++: Generalized gradient-based visual explanations for deep convolutional networks. In *2018 IEEE Winter Conference on Applications of Computer Vision (WACV)*, pages 839–847, 2018. 4
- [5] Ting Chen, Simon Kornblith, Mohammad Norouzi, and Geoffrey Hinton. A simple framework for contrastive learning of visual representations. In *International conference on machine learning*, pages 1597–1607. PMLR, 2020. 2
- [6] Xinlei Chen and Kaiming He. Exploring simple siamese representation learning. In *Proceedings of the IEEE/CVF conference on computer vision and pattern recognition*, pages 15750–15758, 2021. 2
- [7] Xinlei Chen, Haoqi Fan, Ross Girshick, and Kaiming He. Improved Baselines with Momentum Contrastive Learning. *arXiv e-prints*, art. arXiv:2003.04297, 2020. 2, 4
- [8] Xinlei Chen, Saining Xie, and Kaiming He. An empirical study of training self-supervised vision transformers. In *Proceedings of the IEEE/CVF International Conference on Computer Vision (ICCV)*, pages 9640–9649, 2021. 2, 4, 5
- [9] Bowen Cheng, Ross Girshick, Piotr Dollár, Alexander C Berg, and Alexander Kirillov. Boundary iou: Improving object-centric image segmentation evaluation. In *Proceedings of the IEEE/CVF Conference on Computer Vision and Pattern Recognition*, pages 15334–15342, 2021. 7
- [10] Ching-Yao Chuang, Joshua Robinson, Yen-Chen Lin, Antonio Torralba, and Stefanie Jegelka. Debaised contrastive learning. *Advances in neural information processing systems*, 33:8765–8775, 2020. 2
- [11] Adam Coates, Andrew Y. Ng, and Honglak Lee. An analysis of single-layer networks in unsupervised feature learning. *international conference on artificial intelligence and statistics*, 2011. 5
- [12] Alexey Dosovitskiy, Jost Tobias Springenberg, Martin Riedmiller, and Thomas Brox. Discriminative unsupervised feature learning with convolutional neural networks. *Advances in neural information processing systems*, 27, 2014. 2
- [13] Alexey Dosovitskiy, Lucas Beyer, Alexander Kolesnikov, Dirk Weissenborn, Xiaohua Zhai, Thomas Unterthiner, Mostafa Dehghani, Matthias Minderer, Georg Heigold, Sylvain Gelly, Jakob Uszkoreit, and Neil Houlsby. An image is worth 16x16 words: Transformers for image recognition at scale. *ICLR*, 2021. 5
- [14] Spyros Gidaris, Praveer Singh, and Nikos Komodakis. Unsupervised representation learning by predicting image rotations. In *International Conference on Learning Representations*, 2018. 2
- [15] Jean-Bastien Grill, Florian Strub, Florent Altché, Corentin Tallec, Pierre Richemond, Elena Buchatskaya, Carl Doersch, Bernardo Avila Pires, Zhaohan Guo, Mohammad Gheshlaghi Azar, et al. Bootstrap your own latent—a new approach to self-supervised learning. *Advances in neural information processing systems*, 33:21271–21284, 2020. 2
- [16] Kaiming He, Xiangyu Zhang, Shaoqing Ren, and Jian Sun. Deep residual learning for image recognition. In *Proceedings of the IEEE conference on computer vision and pattern recognition*, pages 770–778, 2016. 5
- [17] Kaiming He, Haoqi Fan, Yuxin Wu, Saining Xie, and Ross Girshick. Momentum contrast for unsupervised visual representation learning. In *Proceedings of the IEEE/CVF conference on computer vision and pattern recognition*, pages 9729–9738, 2020. 2, 4
- [18] Kaiming He, Xinlei Chen, Saining Xie, Yanghao Li, Piotr Dollár, and Ross Girshick. Masked autoencoders are scalable vision learners. In *Proceedings of the IEEE/CVF conference on computer vision and pattern recognition*, pages 16000–16009, 2022. 7
- [19] Kunzhe Huang, Yiming Li, Baoyuan Wu, Zhan Qin, and Kui Ren. Backdoor defense via decoupling the training process. In *International Conference on Learning Representations*, 2021. 3

- [20] Ashish Jaiswal, Ashwin Ramesh Babu, Mohammad Zaki Zadeh, Debapriya Banerjee, and Fillia Makedon. A survey on contrastive self-supervised learning. *Technologies*, 9(1): 2, 2020. 1
- [21] Jinyuan Jia, Yupei Liu, and Neil Zhenqiang Gong. Badencoder: Backdoor attacks to pre-trained encoders in self-supervised learning. In *2022 IEEE Symposium on Security and Privacy (SP)*, pages 2043–2059. IEEE, 2022. 3
- [22] Peng-Tao Jiang, Chang-Bin Zhang, Qibin Hou, Ming-Ming Cheng, and Yunchao Wei. Layercam: Exploring hierarchical class activation maps for localization. *IEEE Transactions on Image Processing*, 30:5875–5888, 2021. 4
- [23] Jacob Devlin Ming-Wei Chang Kenton and Lee Kristina Toutanova. Bert: Pre-training of deep bidirectional transformers for language understanding. In *Proceedings of NAACL-HLT*, pages 4171–4186, 2019. 2
- [24] Diederik P Kingma and Max Welling. Auto-encoding variational bayes. *arXiv preprint arXiv:1312.6114*, 2013.
- [25] Soroush Abbasi Koohpayegani, Ajinkya Tejankar, and Hamed Pirsiavash. Mean shift for self-supervised learning. In *Proceedings of the IEEE/CVF International Conference on Computer Vision (ICCV)*, pages 10326–10335, 2021. 2
- [26] Rayan Krishnan, Pranav Rajpurkar, and Eric J Topol. Self-supervised learning in medicine and healthcare. *Nature Biomedical Engineering*, 6(12):1346–1352, 2022. 1
- [27] Changjiang Li, Ren Pang, Zhaohan Xi, Tianyu Du, Shouling Ji, Yuan Yao, and Ting Wang. An embarrassingly simple backdoor attack on self-supervised learning. In *Proceedings of the IEEE/CVF International Conference on Computer Vision*, pages 4367–4378, 2023. 3
- [28] Shaofeng Li, Minhui Xue, Benjamin Zi Hao Zhao, Haojin Zhu, and Xinpeng Zhang. Invisible backdoor attacks on deep neural networks via steganography and regularization. *IEEE Transactions on Dependable and Secure Computing*, 18(5): 2088–2105, 2020. 6
- [29] Min Liu, Alberto Sangiovanni-Vincentelli, and Xiangyu Yue. Beating backdoor attack at its own game. In *Proceedings of the IEEE/CVF International Conference on Computer Vision*, pages 4620–4629, 2023. 2, 4
- [30] Xiao Liu, Fanjin Zhang, Zhenyu Hou, Li Mian, Zhaoyu Wang, Jing Zhang, and Jie Tang. Self-supervised learning: Generative or contrastive. *IEEE transactions on knowledge and data engineering*, 35(1):857–876, 2021. 1
- [31] James B McQueen. Some methods of classification and analysis of multivariate observations. In *Proc. of 5th Berkeley Symposium on Math. Stat. and Prob.*, pages 281–297, 1967. 4
- [32] Rui Min, Zeyu Qin, Li Shen, and Minhao Cheng. Towards stable backdoor purification through feature shift tuning. In *Thirty-seventh Conference on Neural Information Processing Systems*, 2023. 3
- [33] Ishan Misra and Laurens van der Maaten. Self-supervised learning of pretext-invariant representations. In *Proceedings of the IEEE/CVF conference on computer vision and pattern recognition*, pages 6707–6717, 2020. 1
- [34] Bingxu Mu, Zhenxing Niu, Le Wang, Xue Wang, Qiguang Miao, Rong Jin, and Gang Hua. Progressive backdoor erasing via connecting backdoor and adversarial attacks. In *Proceedings of the IEEE/CVF Conference on Computer Vision and Pattern Recognition*, pages 20495–20503, 2023. 2, 4
- [35] Mehdi Noroozi and Paolo Favaro. Unsupervised learning of visual representations by solving jigsaw puzzles. In *ECCV*, 2016. 2
- [36] Lu Pang, Tao Sun, Haibin Ling, and Chao Chen. Backdoor cleansing with unlabeled data. In *Proceedings of the IEEE/CVF Conference on Computer Vision and Pattern Recognition*, pages 12218–12227, 2023. 2, 4
- [37] Adam Paszke, Sam Gross, Francisco Massa, Adam Lerer, James Bradbury, Gregory Chanan, Trevor Killeen, Zeming Lin, Natalia Gimelshein, Luca Antiga, et al. Pytorch: An imperative style, high-performance deep learning library. *Advances in neural information processing systems*, 32, 2019. 12
- [38] Xiangyu Qi, Tinghao Xie, Jiachen T Wang, Tong Wu, Saeed Mahloujifar, and Prateek Mittal. Towards a proactive {ML} approach for detecting backdoor poison samples. In *32nd USENIX Security Symposium (USENIX Security 23)*, pages 1685–1702, 2023. 2, 4
- [39] Alec Radford, Jong Wook Kim, Chris Hallacy, Aditya Ramesh, Gabriel Goh, Sandhini Agarwal, Girish Sastry, Amanda Askell, Pamela Mishkin, Jack Clark, et al. Learning transferable visual models from natural language supervision. In *International conference on machine learning*, pages 8748–8763. PMLR, 2021. 3
- [40] Shaoqing Ren, Kaiming He, Ross Girshick, and Jian Sun. Faster r-cnn: Towards real-time object detection with region proposal networks. *Advances in neural information processing systems*, 28, 2015. 7
- [41] Olga Russakovsky, Jia Deng, Hao Su, Jonathan Krause, Sanjeev Satheesh, Sean Ma, Zhiheng Huang, Andrej Karpathy, Aditya Khosla, Michael Bernstein, Alexander C. Berg, and Li Fei-Fei. ImageNet Large Scale Visual Recognition Challenge. *International Journal of Computer Vision (IJCV)*, 115 (3):211–252, 2015. 5
- [42] Aniruddha Saha, Akshayvarun Subramanya, and Hamed Pirsiavash. Hidden trigger backdoor attacks. In *Proceedings of the AAAI conference on artificial intelligence*, pages 11957–11965, 2020. 5
- [43] Aniruddha Saha, Ajinkya Tejankar, Soroush Abbasi Koohpayegani, and Hamed Pirsiavash. Backdoor attacks on self-supervised learning. In *Proceedings of the IEEE/CVF Conference on Computer Vision and Pattern Recognition*, pages 13337–13346, 2022. 2, 3, 5
- [44] Madeline C Schiappa, Yogesh S Rawat, and Mubarak Shah. Self-supervised learning for videos: A survey. *ACM Computing Surveys*, 55(13s):1–37, 2023. 1
- [45] Ramprasaath R. Selvaraju, Michael Cogswell, Abhishek Das, Ramakrishna Vedantam, Devi Parikh, and Dhruv Batra. Grad-cam: Visual explanations from deep networks via gradient-based localization. In *2017 IEEE International Conference on Computer Vision (ICCV)*, pages 618–626, 2017. 2, 3, 4, 8, 12
- [46] Anshul Shah, Suvrit Sra, Rama Chellappa, and Anoop Cherian. Max-margin contrastive learning. In *Proceedings of*

- the AAAI Conference on Artificial Intelligence*, pages 8220–8230, 2022. [2](#)
- [47] Mingjie Sun, Siddhant Agarwal, and J Zico Kolter. Poisoned classifiers are not only backdoored, they are fundamentally broken. *arXiv preprint arXiv:2010.09080*, 2020. [5](#)
- [48] Guanhong Tao, Zhenting Wang, Shiwei Feng, Guangyu Shen, Shiqing Ma, and Xiangyu Zhang. Distribution preserving backdoor attack in self-supervised learning. In *2024 IEEE Symposium on Security and Privacy (SP)*, pages 29–29. IEEE Computer Society, 2023. [3](#)
- [49] Ajinkya Tejankar, Maziar Sanjabi, Qifan Wang, Sinong Wang, Hamed Firooz, Hamed Pirsiavash, and Liang Tan. Defending against patch-based backdoor attacks on self-supervised learning. In *2023 IEEE/CVF Conference on Computer Vision and Pattern Recognition (CVPR)*, pages 12239–12249, 2023. [1](#), [2](#), [3](#), [4](#), [5](#), [12](#)
- [50] Yonglong Tian, Dilip Krishnan, and Phillip Isola. Contrastive multiview coding. In *Computer Vision—ECCV 2020: 16th European Conference, Glasgow, UK, August 23–28, 2020, Proceedings, Part XI 16*, pages 776–794. Springer, 2020. [5](#)
- [51] Haofan Wang, Zifan Wang, Mengnan Du, Fan Yang, Zijian Zhang, Sirui Ding, Piotr Mardziel, and Xia Hu. Score-cam: Score-weighted visual explanations for convolutional neural networks. In *2020 IEEE/CVF Conference on Computer Vision and Pattern Recognition Workshops (CVPRW)*, pages 111–119, 2020. [4](#)
- [52] Zhirong Wu, Yuanjun Xiong, Stella X Yu, and Dahua Lin. Unsupervised feature learning via non-parametric instance discrimination. In *Proceedings of the IEEE conference on computer vision and pattern recognition*, pages 3733–3742, 2018. [2](#)
- [53] Qiuling Xu, Guanhong Tao, Jean Honorio, Yingqi Liu, Shengwei An, Guangyu Shen, Siyuan Cheng, and Xiangyu Zhang. Medic: Remove model backdoors via importance driven cloning. In *Proceedings of the IEEE/CVF Conference on Computer Vision and Pattern Recognition*, pages 20485–20494, 2023. [3](#)
- [54] Zhilin Yang, Zihang Dai, Yiming Yang, Jaime Carbonell, Russ R Salakhutdinov, and Quoc V Le. Xlnet: Generalized autoregressive pretraining for language understanding. *Advances in neural information processing systems*, 32, 2019. [2](#)
- [55] Yuanshun Yao, Huiying Li, Haitao Zheng, and Ben Y Zhao. Latent backdoor attacks on deep neural networks. In *Proceedings of the 2019 ACM SIGSAC conference on computer and communications security*, pages 2041–2055, 2019. [6](#)
- [56] Yuning You, Tianlong Chen, Yongduo Sui, Ting Chen, Zhangyang Wang, and Yang Shen. Graph contrastive learning with augmentations. *Advances in neural information processing systems*, 33:5812–5823, 2020. [2](#)
- [57] Richard Zhang, Phillip Isola, and Alexei A Efros. Colorful image colorization. In *ECCV*, 2016. [2](#)
- [58] Zaixi Zhang, Qi Liu, Zhicai Wang, Zepu Lu, and Qingyong Hu. Backdoor defense via deconfounded representation learning. In *Proceedings of the IEEE/CVF Conference on Computer Vision and Pattern Recognition*, pages 12228–12238, 2023. [3](#)
- [59] Liuwan Zhu, Rui Ning, Cong Wang, Chunsheng Xin, and Hongyi Wu. Gangsweep: Sweep out neural backdoors by gan. In *Proceedings of the 28th ACM International Conference on Multimedia*, pages 3173–3181, 2020. [6](#)
- [60] Mingli Zhu, Shaokui Wei, Hongyuan Zha, and Baoyuan Wu. Neural polarizer: A lightweight and effective backdoor defense via purifying poisoned features. In *Thirty-seventh Conference on Neural Information Processing Systems*, 2023. [3](#)

A. Preliminary: Heuristic Search Strategy used in Section 4.3

In Section 4.3, to improve the efficiency and utilize the clustering information of images, we adopt a heuristic search strategy following [49] to iteratively compute poison scores for a part of (not all) images in \mathbf{X} . To make our paper self-contained and facilitate the comprehension of experimental results, we introduce the algorithm in this section. More details can be found in [49] and our released code.

At every iteration, we first compute the poison scores of s randomly selected samples per cluster and use the sums to represent the poison scores of clusters. Since clusters with lower poison scores are less likely to be poisoned, we then remove a fraction r of the clusters with the least poison scores and will not compute poison scores for images in these clusters. After several iterations, all clusters are removed, and a part of images in \mathbf{X} are scored during the iterative procedure. Finally, we take the top- k scored images with the highest poison scores to form a poison set \mathbf{X}^P . This poison set will be utilized to train a classifier of poisonous samples. In this heuristic algorithm, the number of scored images is unfixed.

B. Implementation Details

We utilize PyTorch [37] to implement all experiments on four GeForce RTX 3090 GPUs. We employed the following parameters for PoisonCAM on ImageNet-100 as same as PatchSearch: a cluster count of $l = 1000$, the number of the flip test set is set as 1000, samples per cluster $s = 2$, and removal of $r = 25\%$ of candidate clusters after each iteration. The search window size was set to $w = 60$, using a complete sampling approach. This method typically involves searching through approximately 8,000 images on ImageNet-100. For training the poison classifier, we sample top-20 poisonous images (i.e., $|\mathbf{X}^P| = 20$) and remove the top 10% poisonous samples in \mathbf{X} to reduce noise in the poison classification set $\bar{\mathbf{X}}$. Besides, we set the number of masks as $B = 256$.

C. Additional Experiments

C.1. Detailed Results of Poisonous Image Detection

In this section, we list detailed results for poisonous image detection. As shown in Table 4, our PoisonCAM significantly outperforms PatchSearch for defending every category except target category *tabby cat* on ImageNet-100 with poison rate 1.0%. These results demonstrate that PoisonCAM can enhance the accuracy of detecting poisonous images while reducing the number of erroneously removed benign samples. As a result, PoisonCAM can facilitate more comprehensive training, leading to improved performance of the Self-Supervised Learning (SSL) models.

Table 3. **The attack effectiveness throughout the backdoored SSL process.** We evaluated the attack effectiveness using poisoned data to train the self-supervised model with different training epochs. We test the accuracy and false positive rates of the model on clean and poisoned data after fine-tuning on downstream classification tasks using clean datasets. (poison rate 0.5%, target category “laptop” and “goose”). The results show a strong correlation between the effectiveness of the attack and the model performance before 100 epochs.

Epoch	laptop				goose			
	Clean Data		Poison Data		Clean Data		Poison Data	
	Acc	FP	Acc	FP	Acc	FP	Acc	FP
20	24.4	47	18.7	114	24.5	56	18.2	115
40	38.5	44	31.8	416	39.0	39	31.7	181
60	51.8	45	27.8	2390	52.2	30	41.3	566
80	59.4	44	33.3	2368	59.8	17	46.7	705
100	64.1	40	38.9	2238	64.2	16	46.6	1223
120	67.1	39	42.4	2112	66.7	12	46.0	1467
140	68.2	38	40.8	2325	68.3	13	47.0	1485
160	69.0	46	39.5	2492	69.0	12	48.1	1420
180	69.4	43	38.6	2533	69.2	10	42.9	1888
200	69.2	43	38.0	2593	69.4	11	44.7	1758

C.2. More Trigger Attention Maps of Different Target Categories

In this section, we show more trigger attention maps of different target categories to further investigate the search processes of two defenders, PoisonCAM and PatchSearch. Both methods generate trigger attention maps for images and select the hottest regions as the candidate triggers. PatchSearch adopts Grad-CAM [45] to compute the trigger attention, while we propose a Cluster Activation Masking method to solve this problem. In Figures 8, 9, 10, we visualize more cases of trigger attention maps generated by PoisonCAM and PatchSearch on ImageNet-100 (poison rate 0.5%) with the target categories “tabby cat”, “ambulance” and “pickup truck”. Our method can always accurately locate the backdoor triggers contained in these images, while PatchSearch focuses on more dispersed and maybe irrelevant regions. These results further demonstrate that our PoisonCAM can significantly improve the detection accuracy of the injected backdoor trigger, which is fundamental for defending against SSL backdoor attacks.

C.3. Analysis of Backdoored SSL Process

In our assessment of the backdoored SSL process on ImageNet-100 with a poison rate of 0.5%, we conduct a thorough investigation into the correlation between the overall model performance, as measured by Clean Data Acc, and the attack effectiveness, as measured by the Patched Data FP. As shown in Table 3, our findings indicate that in the initial epochs ($epoch \leq 40$), attack effectiveness has a strong correlation with overall model performance.

Table 4. **Poison detection results.** We compared the results of using both methods for cleaning poisoned data at the data level. *Total Rem.* denotes the total removed samples.

Attack Target		PatchSearch			PoisonCAM		
Dataset	Target Category	Total Rem.	Recall \uparrow	Precision \uparrow	Total Rem.	Recall \uparrow	Precision \uparrow
ImageNet-100 (poison rate 0.5%)	rottweiler	8449	97.1	7.5	1556	99.5	41.6
	tabby cat	11341	99.2	5.7	2314	99.8	28.0
	ambulance	13212	31.5	1.6	3509	98.5	18.2
	pickup truck	16523	96.8	3.8	921	98.5	69.5
	laptop	14944	68.5	3.0	1245	98.2	51.2
	goose	14002	99.1	4.6	844	99.1	76.3
	pirate ship	18421	53.5	1.6	1924	96.1	27.9
	gas mask	4785	99.7	13.5	1457	99.5	44.4
	vacuum cleaner	6600	98.9	9.7	806	98.0	79.0
	American lobster	19798	99.7	3.3	1132	99.4	57.1
	average	12807.5	84.4	5.4	1570.8	98.7	49.3
ImageNet-100 (poison rate 1.0%)	rottweiler	20585	99.5	6.3	2083	99.6	62.2
	tabby cat	3806	99.8	34.1	5106	99.5	25.3
	ambulance	14627	96.4	8.6	1980	97.5	64.0
	pickup truck	7918	99.6	16.4	1937	99.4	66.7
	laptop	7918	98.2	21.7	1767	99.6	73.3
	goose	34793	99.5	3.7	1517	98.9	84.8
	pirate ship	10102	99.5	11.0	1925	98.2	57.0
	gas mask	6816	99.2	18.7	1961	99.7	66.1
	vacuum cleaner	2023	98.8	63.5	1696	99.5	76.3
	American lobster	5194	99.8	25.0	1896	98.8	67.8
	average	11174.9	99.0	20.9	2186.8	99.1	64.4
STL-10 (poison rate 5.0%)	bird	306	98.8	80.7	295	98.8	83.7
	car	1755	100.0	14.2	441	98.4	55.8
	deer	261	96.8	92.7	260	100.0	96.2
	average	744.0	98.5	62.5	332.0	99.1	78.6

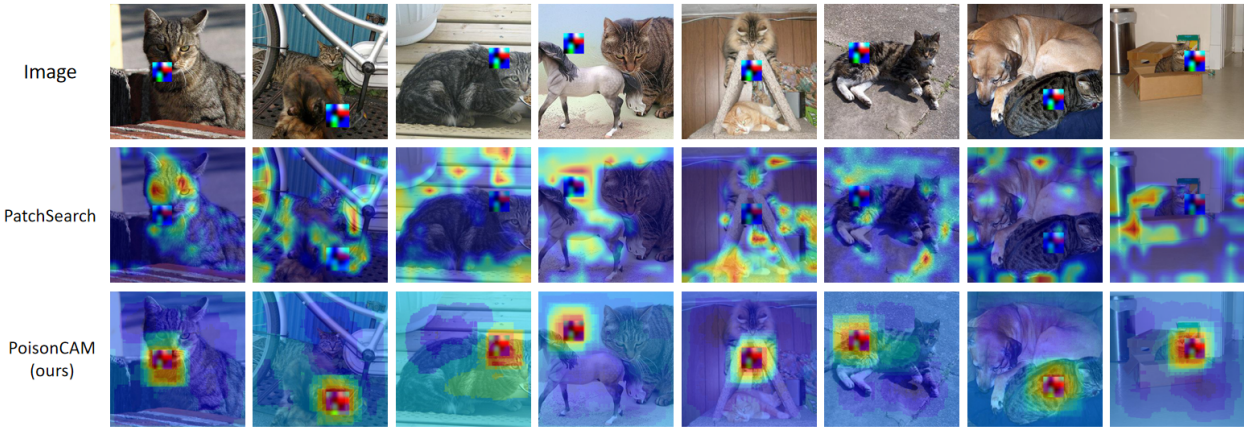


Figure 8. Visualization of trigger attention maps generated by PatchSearch and our PoisonCAM on ImageNet-100 (poison rate 0.5%, target category “tabby cat”).

Although this correlation is not as stringent in later epochs, the attack effectiveness still maintains its overall magnitude. These observations suggest that, when training a model for defense, achieving convergence may not be necessary. Instead, it is sufficient to train the model until the attack ef-

fectiveness is comparable to that of the fully trained model in overall magnitude.



Figure 9. Visualization of trigger attention maps generated by PatchSearch and our PoisonCAM on ImageNet-100 (poison rate 0.5%, target category “ambulance”).



Figure 10. Visualization of trigger attention maps generated by PatchSearch and our PoisonCAM on ImageNet-100 (poison rate 0.5%, target category “pickup truck”).

C.4. Hyper-parameter Sensitivity Study

In this section, we analyze hyper-parameter sensitivity studies on window size w of masks and the cluster count of l on ImageNet-100 with poison rate 0.5%, target category “rotweiler”.

Window size w of masks. As shown in Figure 11, we vary window size w of masks from 40 to 80, where Acc measures if any part of the trigger is contained in the retrieved window. We have the following observations: (1) While increasing w , the IoU of the detected candidate triggers sharply drops for the reason of more trigger-related regions in candidate triggers. (2) CR and Precision first increase and then relatively drop while w increases, which demonstrates that our PoisonCAM can accurately search the triggers with an appropriate w . (3) The recall performs relatively stable, which demonstrates the effectiveness of

our method. We empirically set $w = 60$ in our method.

Number l of clusters. As shown in Figure 12, we vary the cluster number l in k -means algorithm from 100 to 2000 and have the following observations: (1) While increasing l , the Acc of the detected candidate triggers first increases and then becomes relatively stable, and the IoU and CR increase first and then fluctuate. These results demonstrate that a large cluster count of l can detect more candidate images with poisonous triggers. (2) The total processing time consistently increases and the average processing time performs relatively stable while the cluster count of l increases. The system will spend more calculating time with a larger cluster count of l . To conclude, an appropriate value of l should be chosen to balance the performance and time costs. We empirically set $l = 1000$.

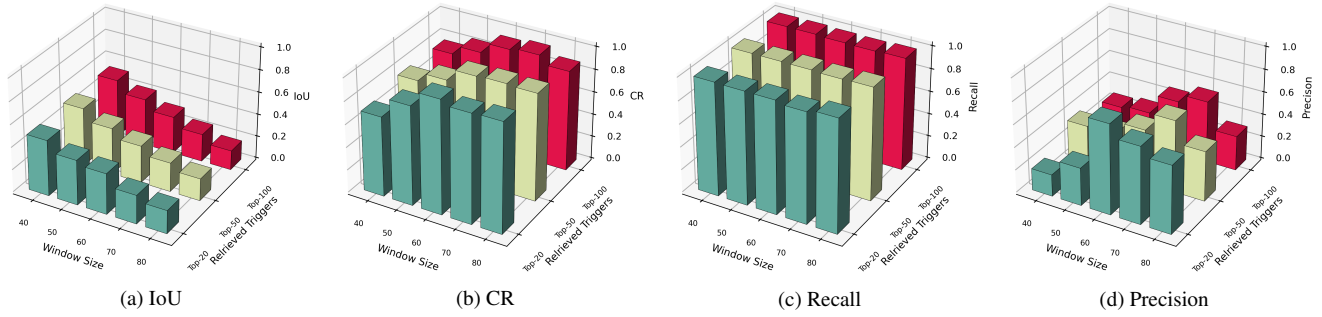


Figure 11. Hyper-parameter sensitivity study on the window size w of masks on ImageNet-100 (poison rate 0.5%, target category “rottweiler”). (a-b) IoU and CR of the detected candidate triggers. (c-d) Recall and precision of the trained poison classifier.

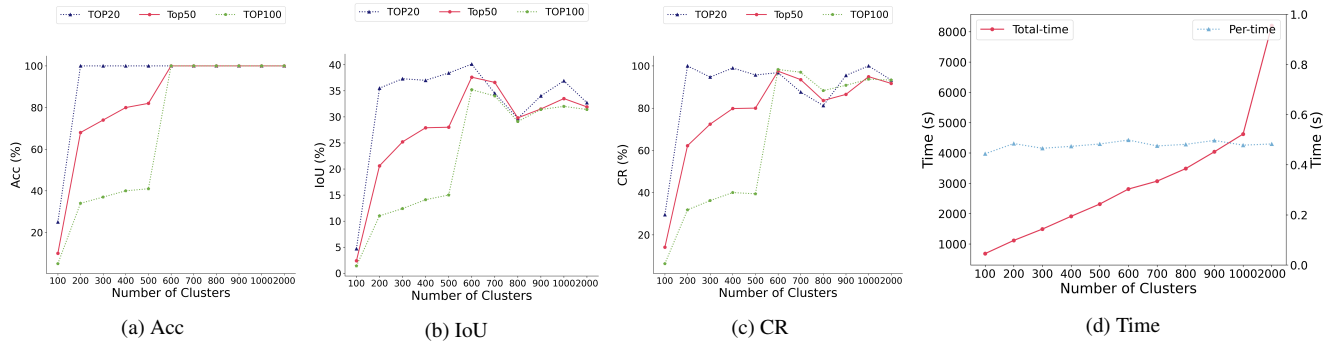


Figure 12. Hyper-parameter sensitivity study on the cluster count of l on ImageNet-100 (poison rate 0.5%, target category “rottweiler”). (a-c) Acc, IoU, and CR of the detected candidate triggers. (d) Total processing time and average processing time per image of candidate trigger detection.

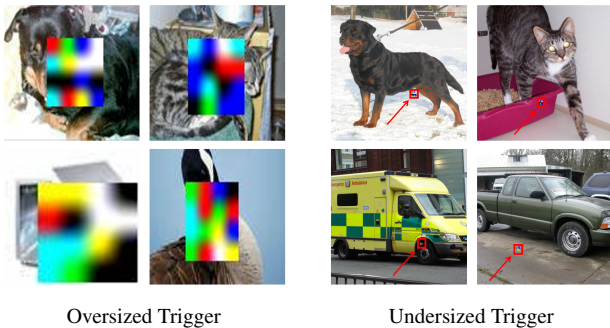


Figure 13. The Poisoned Classifier Misses Examples during the Filtering Stage.

C.5. Analysis of Failure Examples

To conduct a comprehensive analysis of our proposed method and promote further advances in related areas, we analyze the typical failure examples in this section.

C.5.1 Undetected Poisoned Samples

We explore the common characteristics among these undetected poisoned samples with the poison classifier discussed

in Section 4.4. As shown in Figure 13, the poison classifier wrongly recognizes these oversized and undersized poisonous images as clean images. The results show the limitation of the poison classifier.

C.5.2 Trigger Search Errors

Though our PoisonCAM achieves high recall and precision in the poisonous image search stage discussed in Sections 4.2 and 4.3, there still are a few search errors. As shown in Figure 14, we can have the following observations: (1) **Image resembling the trigger.** When some pixels in the candidate image are similar to the backdoor trigger. (2) **Image corrupted by the trigger.** Some triggers are oversized when pasted to form poisonous images, which are hard to search. (3) **Image with the analogous trigger.** The features of some images like honeycombs are similar to the backdoor trigger.



Figure 14. During the process of searching for candidate triggers, there are a few instances of search errors, which can be categorized into three types. **(a)** There are cases where some pixels in the image closely resemble the actual trigger. **(b)** The trigger in the image occupies a significant portion. **(c)** Some inherent features present in the image itself can have a significant impact on the model, acting as a natural trigger, such as a pattern resembling a beehive.